Research Square

Preprints are preliminary reports that have not undergone peer review.
They should not be considered conclusive, used to inform clinical practice,
or referenced by the media as validated information.

Covalent Immobilization of Human Serum Catalase on $Fe3O4@SiO_2–NH_2$ Magnetic Nanoparticles: Stability Assessment, Apparent Kinetic Behavior, and Structural Analysis

AHMED Hussain

ahmedchemistry12@gmail.com

University of Tikrit

Wasan Nazhan

University of Tikrit

Research Article

Keywords: Human serum catalase, Enzyme immobilization, Magnetic nanoparticles, $Fe_3O_4@SiO_2–NH_2$, Covalent immobilization, Biocatalytic stability

Posted Date: March 31st, 2026

DOI: https://doi.org/10.21203/rs.3.rs-9260931/v1

License: This work is licensed under a Creative Commons Attribution 4.0 International License.
Read Full License

Additional Declarations: No competing interests reported.

Abstract

Enzyme immobilization on nanostructured supports is frequently used to increase the stability of enzymes and make recovery from reaction medium easier. In this work, glutaraldehyde was used as a coupling agent to covalently immobilize pure human serum catalase onto amine-functionalized magnetic nanoparticles (Fe_3O_4@SiO_2–NH_2). Fourier transform infrared spectroscopy (FTIR), X-ray diffraction (XRD), scanning electron microscopy (SEM), energy-dispersive X-ray spectroscopy (EDX), and dynamic light scattering (DLS) were used to characterize the resultant support and enzyme-loaded nanocomposite. Successful surface functionalization and enzyme immobilisation were supported by the obtained characterization results. Using hydrogen peroxide as the substrate, catalytic performance was assessed and contrasted with that of the free enzyme. Following immobilization, apparent Michaelis-Menten analysis revealed a little drop in Vmax together with an increase in Km. demonstrating decreased substrate accessibility and the existence of conformational or diffusional restrictions related to covalent attachment to the solid support. Despite these modifications, compared to the free enzyme, the immobilized catalase showed better pH tolerance, heat stability, and storage stability. Furthermore, simple magnetic separation of the immobilized preparation from the reaction medium was made possible by the Fe_3O_4 core. These results suggest that Fe_3O_4@SiO_2–NH_2 offers an appropriate foundation for the creation of magnetically recoverable catalase systems with improved stability.

1. Introduction

Enzymes are widely used as biocatalysts in biochemical environmental and industrial processes because of their high catalytic efficiency and substrate specificity under mild operating conditions. Catalase (EC 1.11.1.6) plays an important protective role in biological systems by rapidly decomposing hydrogen peroxide into water and molecular oxygen. Because of its function, catalase has drawn ongoing attention for antioxidant technologies, biosystems that regulate reactive oxygen species, and catalytic processes that need for the elimination of peroxide.[1]. Nevertheless, the practical use of free catalase is constrained by several well-recognized drawbacks, including limited operational stability, sensitivity to pH and temperature fluctuations, gradual activity loss during storage, and difficulty in recovering the enzyme from reaction media [2, 3]. These limitations reduce process robustness and increase operating costs particularly in systems that require repeated or prolonged use. Accordingly, enzyme immobilization has become an established strategy for improving catalytic stability simplifying separation and extending the functional lifetime of enzyme preparations [4–6]. Magnetic iron oxide nanoparticles are a desirable immobilization platform due to their high surface-to-volume ratio and easy recovery in the presence of an external magnetic field. While amine functionalization produces reactive surface groups that can be connected to proteins via bifunctional cross-linkers like glutaraldehyde coating Fe_3O_4 with silica increases chemical stability and decreases aggregation. [2, 7]. For these reasons, Fe_3O_4@SiO_2–NH_2 nanoparticles represent suitable supports for the preparation of magnetically recoverable and reusable biocatalysts. Even though catalase immobilization has been extensively researched, there are still few reports that specifically address purified human serum catalase

immobilized on Fe_3O_4@SiO_2–NH_2 supports. This limitation is particularly evident in studies that combine apparent kinetic analysis with pH, thermal storage and structural evaluation after immobilization. In order to evaluate the resulting biocatalyst using complementary kinetic stability and physicochemical tests the current study set out to build a covalently immobilized human serum catalase system on Fe_3O_4@SiO_2–NH_2 magnetic nanoparticles. The study further examined how immobilization influenced the apparent catalytic behavior and stability profile of the enzyme preparation [8]. Particular attention was therefore directed toward the effects of immobilization on the apparent Michaelis-Menten parameters as well as on pH, thermal, and storage stability, since these properties are central to practical long-term use. Glutaraldehyde-mediated coupling was employed to attach human serum catalase covalently to the amine-functionalized magnetic support (Fe_3O_4@SiO_2–NH_2) [6, 9]. Structural and physicochemical methods were used to thoroughly characterize the resulting immobilized enzyme system. In addition the apparent kinetic behavior of the immobilized catalase was compared with that of the free enzyme and its pH stability thermal stability storage stability and magnetic recovery potential were investigated [2, 3]. The aim of this work was to assess human serum catalase immobilized on Fe_3O_4@SiO_2–NH_2 as a magnetically recoverable biocatalyst with improved stability characteristics and potential biochemical applicability [10].

2. Materials and Methods

2.1 Ethical considerations

Administrative approval for sample collection was granted by the Deanship of the College of Education for Pure Sciences, University of Tikrit, and the collection of human serum samples was subsequently approved by Baqubah Teaching Hospital. Informed consent was obtained from all participants before sample collection. Administrative approval for sample collection was granted by the Deanship of the College of Education for Pure Sciences, University of Tikrit, and the collection of human serum samples was subsequently approved by Baqubah Teaching Hospital. Informed consent was obtained from all participants before sample collection. All procedures involving human-derived samples were conducted in accordance with institutional requirements and the ethical principles governing research involving human subjects.

2.2 Purified catalase freeze-drying

Following purification, human serum catalase was preserved by freeze-drying to maintain its catalytic activity and structural integrity. Freeze-drying was carried out using a standard protein preservation approach with minor procedural modifications. Because the enzyme samples had already been kept under deep-freezing conditions, a separate pre-freezing step was not required. Primary drying was conducted under reduced pressure for approximately 8 h, followed by secondary drying for 30–60 min to remove residual bound moisture. The resulting dry catalase powder was stored in airtight containers under deep-freezing conditions until further use. Prior to immobilization, the freeze-dried enzyme was

reconstituted in phosphate buffer, and its activity was verified using the standard assay applied throughout this study[11].

2.3 Fe_3O_4 nanoparticle synthesis

Magnetic Fe_3O_4 nanoparticles were synthesized by a chemical co-precipitation method commonly used for iron oxide nanoparticle preparation. Ferric chloride hexahydrate and ferrous chloride tetrahydrate were dissolved in deionized water at a molar ratio of 2:1 under a nitrogen atmosphere. The reaction mixture was heated to 80°C, followed by dropwise addition of aqueous ammonia solution. The resulting black precipitate was magnetically separated, washed thoroughly with deionized water and ethanol, and dried prior to further modification[12].

2.4 $Fe_3O_4@SiO_2$ nanoparticle preparation

Silica coating of Fe_3O_4 nanoparticles was performed using a modified Stöber method to improve surface stability and prevent aggregation. Fe_3O_4 nanoparticles were dispersed in an ethanol–water mixture, followed by the addition of ammonia solution and tetraethyl orthosilicate (TEOS) under continuous stirring. The resulting $Fe_3O_4@SiO_2$ nanoparticles were magnetically separated, washed, and dried under vacuum[13–15].

2.5 Preparation of amine-functionalized $Fe_3O_4@SiO_2–NH_2$ nanoparticles

Surface amine functionalization was carried out using 3-aminopropyltriethoxysilane (APTES) through a silanization procedure. $Fe_3O_4@SiO_2$ nanoparticles were dispersed in ethanol, reacted with APTES under heating and stirring, and subsequently washed and dried to obtain $Fe_3O_4@SiO_2–NH_2$ nanoparticles[16].

2.6 Covalent immobilization of human serum catalase

Using glutaraldehyde as a bifunctional coupling agent, catalase was covalently immobilised onto $Fe_3O_4@SiO_2–NH_2$ nanoparticles. Glutaraldehyde was utilised to first activate the amine-functionalized nanoparticles. The activated support was then incubated with the catalase solution under the selected experimental conditions of pH, temperature, and mixing. Before further analysis, the resultant $Fe_3O_4@SiO_2–NH_2–CAT$ preparation was magnetically separated and repeatedly washed to eliminate unbound or weakly attached enzyme [17, 18].

2.7 Immobilization efficiency, apparent kinetic analysis, and catalase activity assay

Hydrogen peroxide was used as the substrate to test catalase activity. Lineweaver-Burk plots created from the activity data were used to estimate apparent Michaelis-Menten parameters (Km and Vmax). By comparing the catalytic activity of the immobilized preparation with that of the free enzyme at the same substrate concentration under the same test conditions, operational immobilization efficiency was determined [3].

2.8 Studies on pH, temperature, and storage stability

The assay conditions used in this investigation were used to assess the effects of pH, temperature, and storage duration on free and immobilised catalase. The stability profiles of the respective free enzyme and the immobilised preparation were compared using these assays.

2.9 Physicochemical characterization

To verify surface functionalization, enzyme attachment, morphology, and colloidal size behavior, the produced nanoparticles and the immobilized enzyme system were examined using Fourier transform infrared spectroscopy (FTIR), X-ray diffraction (XRD), scanning electron microscopy (SEM), energy-dispersive X-ray spectroscopy (EDX), and dynamic light scattering (DLS). [19].

3. Results and Discussion

3.1 Apparent kinetic behavior of free and immobilized catalase

Using hydrogen peroxide as a substrate, the catalytic activity of free and immobilized human serum catalase was assessed, and Lineweaver–Burk plots were used to estimate the apparent kinetic constants. Free catalase showed high linearity (R^2 = 0.9992), with an apparent Km of around 4×10^{-8} and a Vmax of 650.8 U mL^{-1}, as shown in Table 1 and Figs. 2–3. The apparent Km increased to around 9×10^{-8} after immobilization on Fe_3O_4@SiO_2–NH_2 nanoparticles, but Vmax marginally dropped to 599.3 U mL^{-1} (R^2 = 0.9827). The mild decrease in Vmax is consistent with partial restriction of enzyme mobility rather than full catalytic deactivation, but the increase in apparent Km indicates decreased substrate accessibility and/or diffusional constraints following covalent attachment to solid support. This pattern, which is common for enzymes immobilised on stiff supports, shows that catalase activity was mostly maintained upon attachment to the surface of the nanoparticle. [3, 8].

Table 1. Human serum catalase's apparent kinetic characteristics, both free and immobilised.

Enzyme system	Km (H_2O_2)	Vmax (U mL^{-1})	R^2
Free catalase	≈ 4×10^{-8}	650.8	0.9992
Immobilized catalase (Fe_3O_4@SiO_2–NH_2–CAT)	≈ 9×10^{-8}	599.3	0.9827

3.2 Immobilization Efficiency

The preserved catalytic activity of the immobilized preparation in comparison to the free enzyme across the tested substrate concentrations was used to assess the apparent immobilization effectiveness of catalase on Fe_3O_4@SiO_2–NH_2 nanoparticles. Table 2 and Fig. 4 demonstrate that the efficiency peaked

at the highest substrate concentration (99.23% at 8.82×10^{-3}) and gradually reduced as the substrate concentration decreased, reaching 44.99% at 8.82×10^{-8}. At lower concentrations, where surface-associated kinetic constraints become more apparent, this pattern is consistent with diffusional limitations and decreased effective substrate access. Crucially, the high activity maintained at high substrate concentrations suggests that a significant portion of catalase's catalytic activity was retained during the immobilization process [20].

Table 2
Catalase's apparent immobilization effectiveness on Fe_3O_4@SiO_2–NH_2 nanoparticles.

Substrate concentration [S]	Free catalase activity (IU/L)	Immobilized catalase activity (IU/L)	Immobilization efficiency (%)
8.82×10^{-3}	660.57	655.51	99.23
8.82×10^{-4}	655.20	641.30	97.88
8.82×10^{-5}	650.87	605.45	93.02
8.82×10^{-6}	640.82	550.37	85.88
8.82×10^{-7}	610.52	450.15	73.76
8.82×10^{-8}	490.93	220.92	44.99

3.3 Effect of pH on Catalase Activity

The impact of pH on the catalytic activity of both free and immobilized catalase is depicted in Fig. 5. Given the well-known pH sensitivity of the native enzyme, free catalase showed maximum activity around pH 8 and then decreased under more acidic or strongly alkaline circumstances. The immobilized preparation, on the other hand, showed a wider pH-response profile, with appreciable activity maintained even in highly alkaline circumstances and maximal activity close to pH 10. This change implies that immobilization decreased the degree of pH-induced conformational disruption and created a more protected milieu surrounding the enzyme.[18, 21].

3.4 Thermal stability of free and immobilized catalase

Figure 6 shows the temperature-dependent activity profiles of both free and immobilized catalase. Thermal denaturation of the soluble protein is consistent with the free enzyme's peak activity at 40°C and subsequent abrupt reduction as the temperature rose. The immobilized catalase, on the other hand, demonstrated a wider temperature tolerance and continued to be more active at increasing temperatures, reaching its maximal reaction at about 70°C. Conformational limitation imposed by covalent attachment to the support, which can lessen heat-induced unfolding, is consistent with the enhanced thermal behavior [18].

3.5 Storage Stability

The storage stability of free and immobilized catalase over 168 hours is summarized in Table 3 and Fig. 7. During storage, free catalase activity gradually dropped from 1.06 Units/mg at 24 hours to 0.58 Units/mg at 168 hours. The immobilized preparation, on the other hand, maintained significantly more activity during that time, peaking at 1.18 Unit/mg at 72 hours and staying at 0.95 Unit/mg after 168 hours. These results show that attachment to the Fe_3O_4@SiO_2–NH_2 support enhanced the temporal stability of the enzyme preparation and decreased activity loss during storage [22].

Table 3
Storage stability of free and immobilized catalase

Storage time (h)	Immobilized catalase (Unit/mg)	Free catalase (Unit/mg)
24	1.02	1.06
48	1.08	0.83
72	1.18	0.68
96	1.10	0.60
120	1.05	0.59
144	1.00	0.58
168	0.95	0.58

3.6 Structural and Physicochemical Characterization

3.6.1 FTIR Analysis

Figure 8 shows the FTIR spectrum of Fe_3O_4, Fe_3O_4@SiO_2–NH_2, and Fe_3O_4@SiO_2–NH_2–CAT.

Fe–O stretching vibrations of the magnetite core were identified as the characteristic bands at 570 and 439 cm^{-1} for Fe_3O_4 nanoparticles. Bending and stretching vibrations linked to adsorbed water and surface hydroxyl groups were identified as additional characteristics around 1600 cm^{-1} and 3425 cm^{-1}. The Fe–O band persisted after silica coating and amination, confirming the magnetic core's retention, while bands in the 1000–1100 cm^{-1} area indicated the presence of Si–O–Si bonds connected to the silica shell.

Additional bands in the 1400–1600 cm^{-1} region and broadened high-wavenumber signals after amination and enzyme immobilization were consistent with protein-associated vibrations, surface amine groups, and the formation of the glutaraldehyde-mediated linkage between catalase and the activated support. Overall, effective surface modification and subsequent enzyme immobilization were corroborated by the FTIR results [16, 23, 24].

3.6.2 XRD analysis

Figure 9 displays the X-ray diffraction patterns of Fe_3O_4, Fe_3O_4@SiO_2–NH_2, and Fe_3O_4@SiO_2–NH_2–CAT. Table 4 summarizes the computed crystallite sizes. Fe_3O_4 diffractogram showed the distinctive reflections of crystalline magnetite, with the strongest peak found close to 2θ = 35.86°. The major magnetite reflections were preserved following silica coating and amine functionalization, suggesting that the Fe_3O_4 crystalline phase was preserved following surface modification. The amorphous silica shell is consistent with the appearance of a broad low-intensity feature about 18.44°. The composite continued to display the main magnetite peaks after catalase immobilization, indicating that enzyme loading did not cause the magnetic core to undergo a phase change. It is more reasonable to view changes in peak breadth and the computed crystallite size following coating and immobilization as the result of surface modification and modified coherent scattering domains within the composite material rather than loss of the magnetite structure [14].

Table 4. Apparent crystallite size of Fe_3O_4-based materials estimated from XRD data.

Sample	Main peak (2θ)	Crystallite size (nm)
Fe_3O_4	35.86°	29.78
Fe_3O_4@SiO_2–NH_2	35.98°	10.96
Fe_3O_4@SiO_2–NH_2–CAT	35.59°	13.47

3.6.3 SEM and EDX analysis

SEM micrographs of Fe_3O_4, Fe_3O_4@SiO_2–NH_2, and Fe_3O_4@SiO_2–NH_2–CAT are shown in Fig. 10

Due to their high surface energy and magnetic attraction, the Fe_3O_4 nanoparticles emerged as aggregated quasi-spherical particles. Particle dispersion improved and the surface became more homogeneous following silica coating and amine functionalization. The particles showed significantly rougher surfaces and occasionally bigger aggregates after catalase immobilization, which is consistent with partial agglomeration and enzyme coverage. The corresponding EDX spectra (Fig. 11) confirmed the expected compositional changes at each modification step: following silica coating and amination, the relative Fe signal decreased while Si, C, O, and trace N signals became more noticeable; following enzyme immobilization, the persistence of Si and N along with protein-associated carbon and oxygen signals further supported the successful loading of catalase onto the nanoparticle surface.[14, 25, 26].

3.6.4 DLS analysis

Figure 12 displays the hydrodynamic size distribution of Fe_3O_4@SiO_2–NH_2–CAT nanoparticles as determined by dynamic light scattering. A wide and extremely polydisperse dispersion was indicated by the observed Z-average diameter of 1438.2 nm and the polydispersity index of 0.809. Despite the observation of a population centred about 216.9 nm, the huge Z-average value suggests significant

aggregation in an aqueous medium. Since DLS detects hydrated particles in suspension and is heavily impacted by agglomeration and surface-bound solvent layers, the larger hydrodynamic size in comparison to SEM-derived particle dimensions is expected. Therefore, rather than a narrowly monodisperse colloid, the DLS data support particle association in solution [21, 27, 28] .

4. Conclusions

In this work, glutaraldehyde coupling was used to successfully immobilize pure human serum catalase onto amine-functionalized magnetic Fe_3O_4@SiO_2–NH_2 nanoparticles. According to FTIR, XRD, SEM, EDX, and DLS tests, the resulting immobilized preparation clearly demonstrated surface alteration and enzyme attachment while maintaining the structural characteristics of the magnetic core. Following immobilization, apparent kinetic analysis showed a slight drop in Vmax and a rise in Km, which is consistent with the diffusional and steric restrictions frequently seen for enzymes affixed to rigid supports.

The immobilized catalase showed superior resilience to high temperatures, greater pH tolerance, and better storage stability over 168 hours in comparison to the free enzyme. These modifications suggest that Fe_3O_4@SiO_2–NH_2 can be a useful support for maintaining significant catalytic activity while stabilising human serum catalase. The usage of Fe_3O_4@SiO_2–NH_2 magnetic nanoparticles as a viable platform for creating magnetically recoverable catalase systems is generally supported by the current findings. Overall the present findings support the use of Fe_3O_4@SiO_2–NH_2 magnetic nanoparticles as a suitable platform for the preparation of magnetically recoverable human catalase systems with improved stability characteristics.

Declarations

Competing Interests

The authors declare that they have no known financial or non-financial competing interests.

Competing Interests

The authors have no relevant financial or non-financial interests to disclose.

Ethical approval / informed consent

Human serum samples were collected after institutional and hospital approval, and informed consent was obtained from all participants prior to sample collection.

Funding

The authors received no specific funding for this work.

Author Contribution

Ahmed A. Al Shammari contributed to study conception and design, experimental work, data analysis, and manuscript drafting. Wasan Nazhan Hussein contributed to data interpretation, manuscript review, and final approval of the submitted version. Both authors read and approved the final manuscript.

Acknowledgements

The authors would like to acknowledge the Deanship of the College of Education for Pure Sciences, Tikrit University, for administrative support and facilitation of sample collection procedures. The authors also acknowledge Baqubah Teaching Hospital for its cooperation during sample collection.

Data Availability

The data supporting the findings of this study are available from the corresponding author upon reasonable request.

References

1. Chelikani P, Fita I, Loewen PC (2004) Diversity of Structures and Properties among Catalases. Cell Mol Life Sci 61:192–208. 10.1007/s00018-003-3206-5
2. Datta S, Christena LR, Rajaram YRS (2013) Enzyme Immobilization: An Overview on Techniques and Support Materials. *3 Biotech 3*, 1–9. 10.1007/s13205-012-0071-7
3. Sheldon RA, van Pelt S (2013) Enzyme Immobilisation in Biocatalysis: Why, What and How. Chem Soc Rev 42:6223–6235. 10.1039/c3cs60075k
4. Ansari SA, Husain Q (2012) Potential Applications of Enzymes Immobilized on/in Nano Materials: A Review. Biotechnol Adv 30:512–523. 10.1016/j.biotechadv.2011.09.005
5. Ahmadi P, Tabibiazar M, Roufegarinejad L, Babazadeh A (2020) Development of Behenic Acid-Ethyl Cellulose Oleogel Stabilized Pickering Emulsions as Low Calorie Fat Replacer. Int J Biol Macromol 150:974–981. 10.1016/j.ijbiomac.2019.10.205
6. Mateo C, Palomo JM, Fernandez-Lorente G, Guisan JM, Fernandez-Lafuente R (2007) Improvement of Enzyme Activity, Stability and Selectivity via Immobilization Techniques. Enzyme Microb Technol 40:1451–1463. 10.1016/j.enzmictec.2007.01.018

7. Laurent S, Forge D, Port M (2008) others Magnetic Iron Oxide Nanoparticles: Synthesis, Stabilization, Vectorization, Physicochemical Characterizations, and Biological Applications. Chem Rev 108:2064–2110. 10.1021/cr068445e
8. Ansari SA, Husain Q (2012) Potential Applications of Enzymes Immobilized on/in Nano Materials: A Review. Biotechnol Adv 30:512–523. 10.1016/j.biotechadv.2011.09.005
9. Baird L, Swift S, Llères D, Dinkova-Kostova AT (2014) Monitoring Keap1-Nrf2 Interactions in Single Live Cells. Biotechnol Adv 32:1133–1144. 10.1016/j.biotechadv.2014.03.004
10. Khan MR, Immobilized Enzymes (2021) A Comprehensive Review. Bull Natl Res Cent 45. 10.1186/s42269-021-00649-0
11. Kommineni N, Butreddy A, Sainaga Jyothi VGS, Angsantikul P (2022) Freeze-Drying for the Preservation of Immunoengineering Products. *iScience 25*, 105127. 10.1016/j.isci.2022.105127
12. Dudchenko N, Pawar S, Perelshtein I, Fixler D (2022) Magnetite Nanoparticles: Synthesis and Applications in Optics and Nanophotonics. Mater (Basel) 15. 10.3390/ma15072601
13. Journal C, Chinese OF (2013) □ □ SiO 2 / Fe 3 O 4 □□□□□□□□□□□□□ (. *34*, 2–8
14. Ficai A (2021) Applied Sciences Magnetite-Silica Core / Shell Nanostructures: From Surface Functionalization towards Biomedical Applications — A Review. 1–21
15. Zhang B, Hu C, Xin Y, Li Y, Xie Y, Xing Q, Guo Z, Xue Z, Li D, Zhang G et al (2022) Analysis of Low-Frequency 1/f Noise Characteristics for MoTe2 Ambipolar Field-Effect Transistors. Nanomaterials 12:1–9. 10.3390/nano12081325
16. Mohammed MAA, Chen Z, Li K, Zhang B (2022) The Study of Fe3O4@SiO2-NH2 Nano-Magnetic Composite Modified by Glutaraldehyde to Immobilized Penicillin G Acylase. Turkish J Chem 46:103–115. 10.3906/kim-2103-60
17. Ahmadi P, Tabibiazar M, Roufegarinejad L, Babazadeh A (2020) Development of Behenic Acid-Ethyl Cellulose Oleogel Stabilized Pickering Emulsions as Low Calorie Fat Replacer. Int J Biol Macromol 150:974–981. 10.1016/j.ijbiomac.2019.10.205
18. Goyal P, Mishra V, Dhamija I, Kumar N, Kumar S (2022) Immobilization of Catalase on Functionalized Magnetic Nanoparticles: A Statistical Approach. *3 Biotech 12*, 1–14. 10.1007/s13205-022-03173-8
19. Elizondo-Villarreal N, Verástegui-Domínguez L, Rodríguez-Batista R, Gándara-Martínez E, Alcorta-García A, Martínez-Delgado D, Rodríguez-Castellanos EA, Vázquez-Rodríguez F, Gómez-Rodríguez C (2022) Green Synthesis of Magnetic Nanoparticles of Iron Oxide Using Aqueous Extracts of Lemon Peel Waste and Its Application in Anti-Corrosive Coatings. Mater (Basel) 15. 10.3390/ma15238328
20. Tadesse M, Liu Y (2025) Recent Advances in Enzyme Immobilization: The Role of Artificial Intelligence, Novel Nanomaterials, and Dynamic Carrier Systems. Catalysts 15. 10.3390/catal15060571
21. Singh B (2025) Enzyme Immobilization on Nanomaterials and Their Applications
22. Barbosa LG, Costa TR, Borges IP, Costa MS, Carneiro AC, Borges BC, Silva MJB, Amorim FG, Quinton L, Yoneyama KAG et al (2021) A Comparative Study on the Leishmanicidal Activity of the L-Amino

Acid Oxidases BjussuLAAO-II and BmooLAAO-II Isolated from Brazilian Bothrops Snake Venoms. Int J Biol Macromol 167:267–278. 10.1016/j.ijbiomac.2020.11.146

23. Nasaj M, Farmany A, Shokoohizadeh L, Jalilian FA, Mahjoub R, Roshanaei G, Nourian A, Shayesteh OH, Arabestani M (2024) Vancomycin and Nisin-Modified Magnetic Fe3O4@SiO2 Nanostructures Coated with Chitosan to Enhance Antibacterial Efficiency against Methicillin Resistant Staphylococcus Aureus (MRSA) Infection in a Murine Superficial Wound Model. BMC Chem 18:1–22. 10.1186/s13065-024-01129-y
24. Azarnier SG, Esmkhani M, Dolatkhah Z, Javanshir S (2022) Collagen-Coated Superparamagnetic Iron Oxide Nanoparticles as a Sustainable Catalyst for Spirooxindole Synthesis. Sci Rep 12:1–19. 10.1038/s41598-022-10102-5
25. Aslani E, Abri A, Pazhang MSC (2018) Colloids Surf B Biointerfaces. 10.1016/j.colsurfb.2018.06.022
26. Journal AI, Singh S, Goel T, Singh A, Chugh H, Roy I, Tiwari M, Chandra R (2024) Synthesis and Characterization of Fe 3 O 4 @ SiO 2 @ PDA @ Ag Core – Shell Nanoparticles and Biological Application on Human Lung Cancer Cell Line and Antibacterial Strains. Artif Cells Nanomed Biotechnol 52:46–58. 10.1080/21691401.2023.2295534
27. Bhattacharjee S (2016) DLS and Zeta Potential - What They Are and What They Are Not? J Control Release 235:337–351. 10.1016/j.jconrel.2016.06.017
28. Gama Cavalcante AL, Dari DN, Izaias da Silva Aires F, Carlos de Castro E, dos Moreira K (2024) Sousa dos Santos, J.C. Advancements in Enzyme Immobilization on Magnetic Nanomaterials: Toward Sustainable Industrial Applications. RSC Adv 14:17946–17988. 10.1039/d4ra02939a

Figures

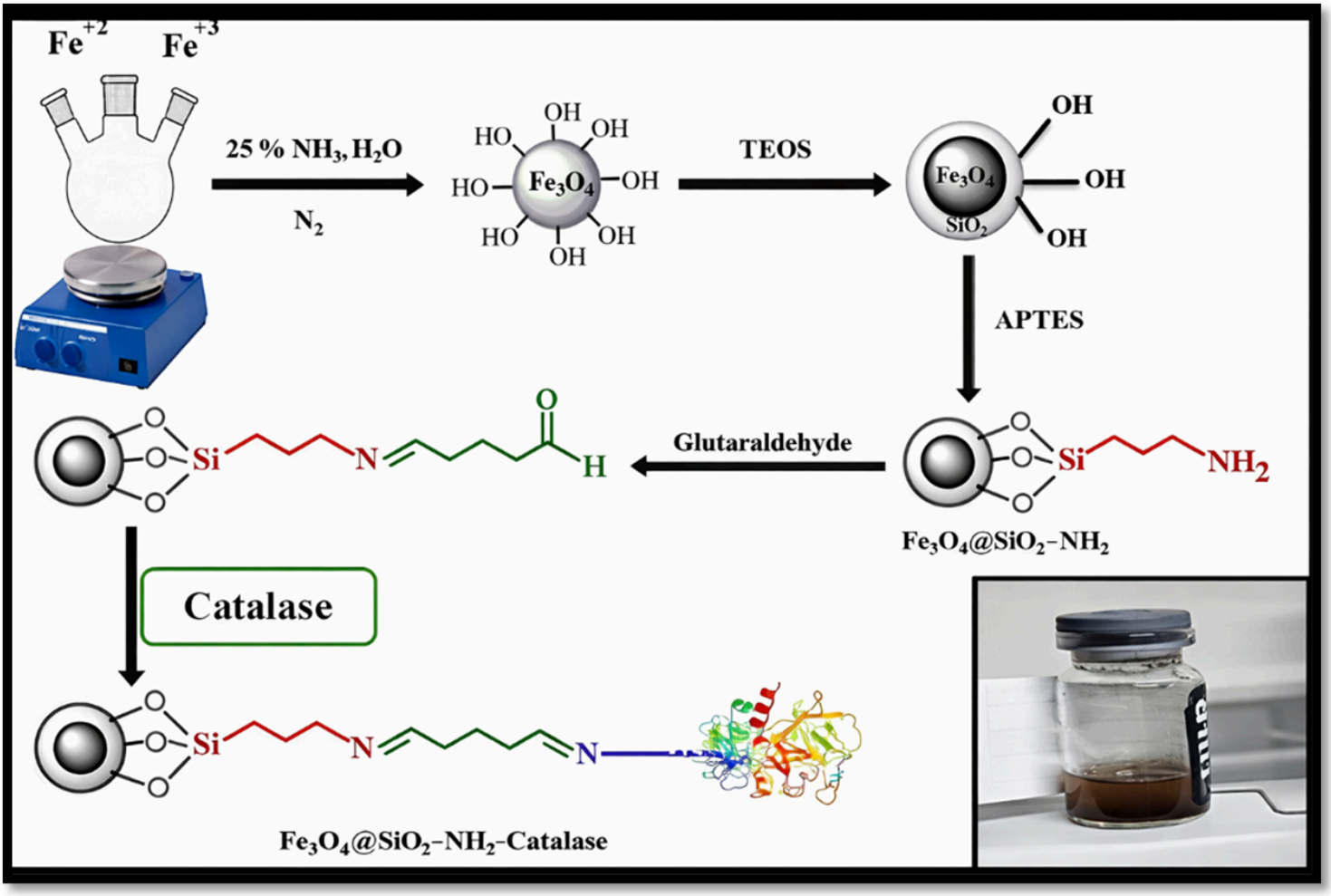


Figure 1

Diagrammatic illustration of human serum catalase immobilization on Fe3O4@SiO_2–NH_2 magnetic nanoparticles.

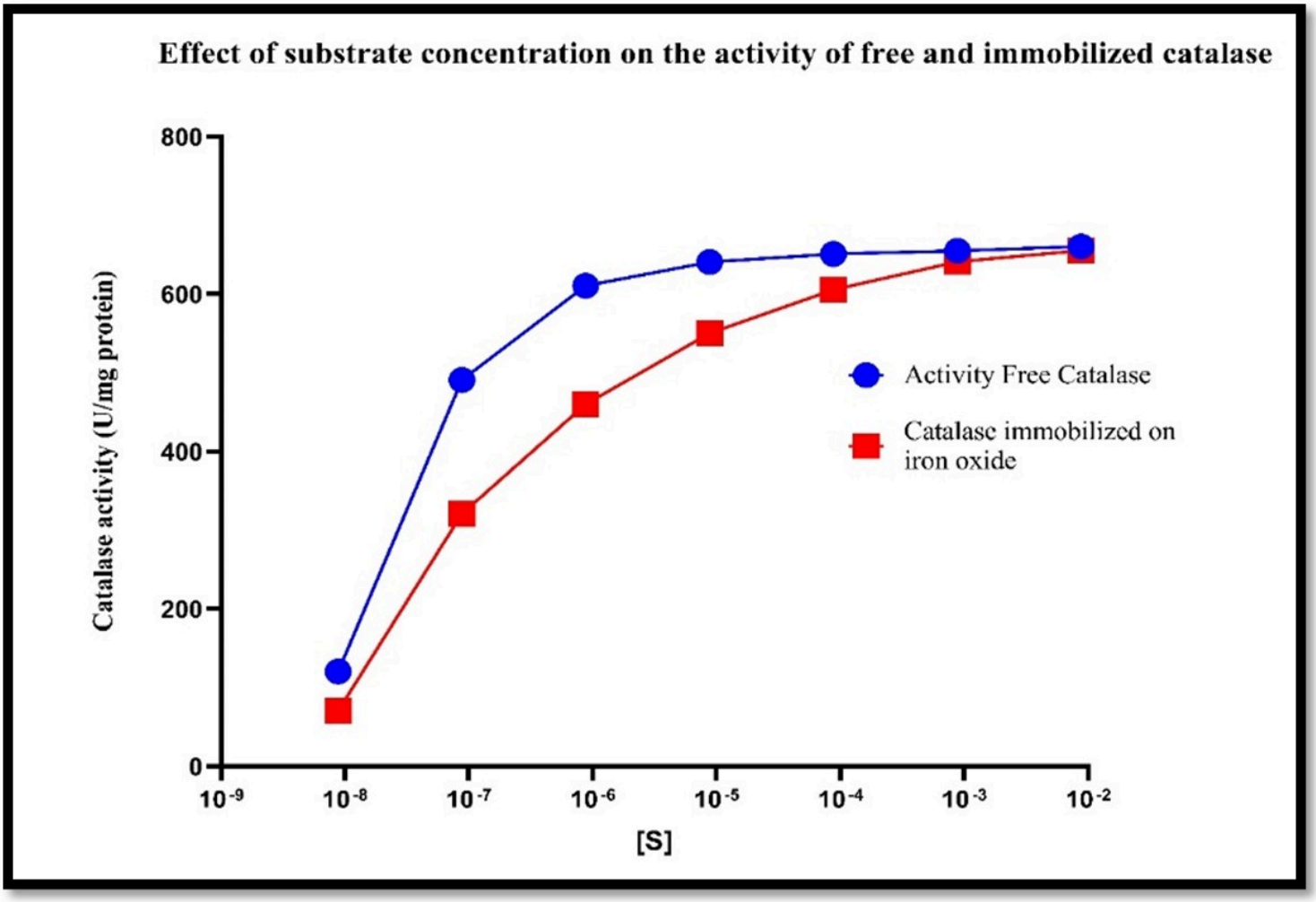


Figure 2

The impact of substrate concentration on both free and immobilised catalase activity.

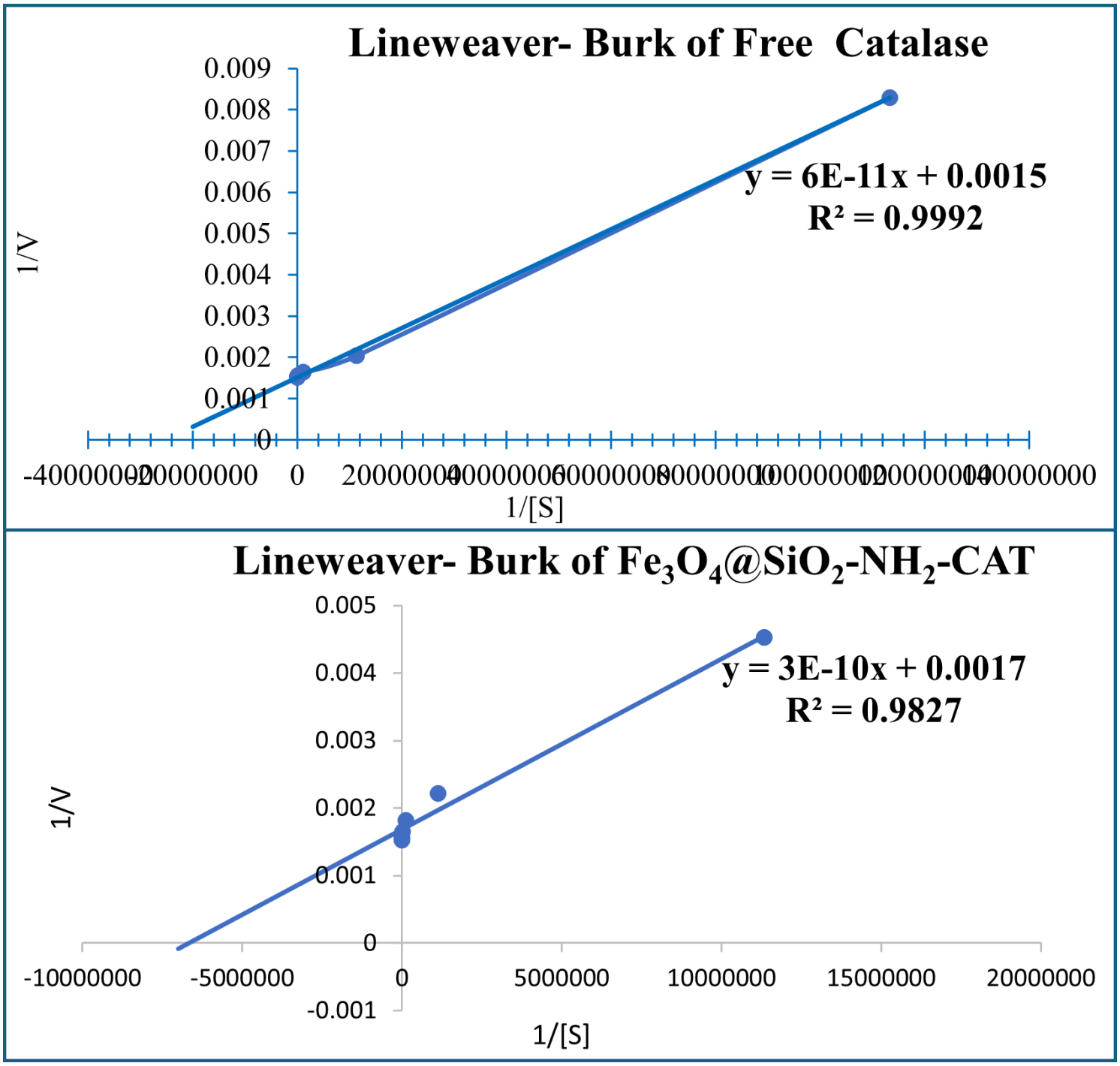


Figure 3

The apparent Km of free catalase and Fe_3O_4@SiO_2–NH_2–CAT are estimated using Lineweaver–Burk plots.

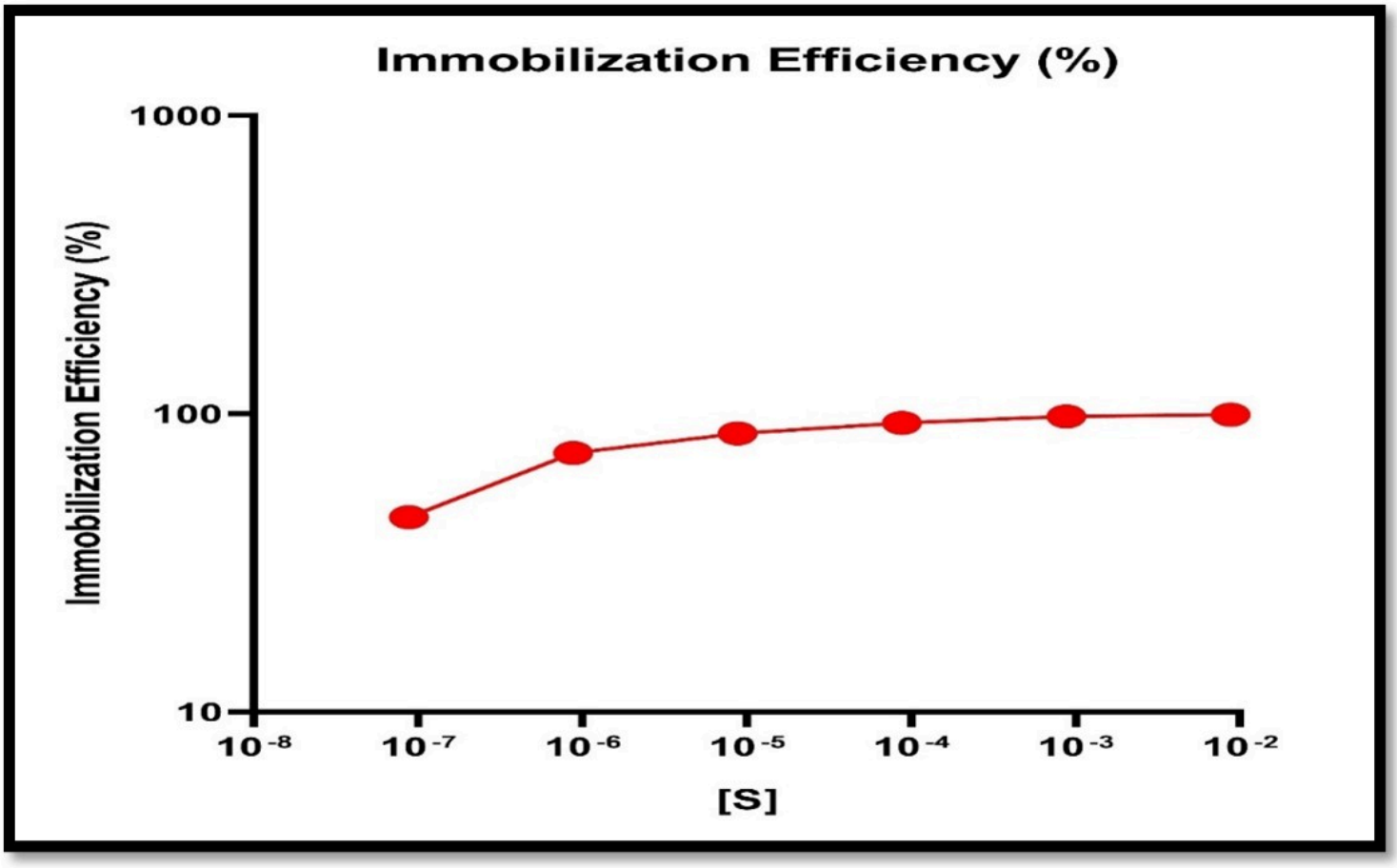


Figure 4

Variation in catalase immobilization efficiency on Fe_3O_4@SiO_2–NH_2 as a function of substrate concentration

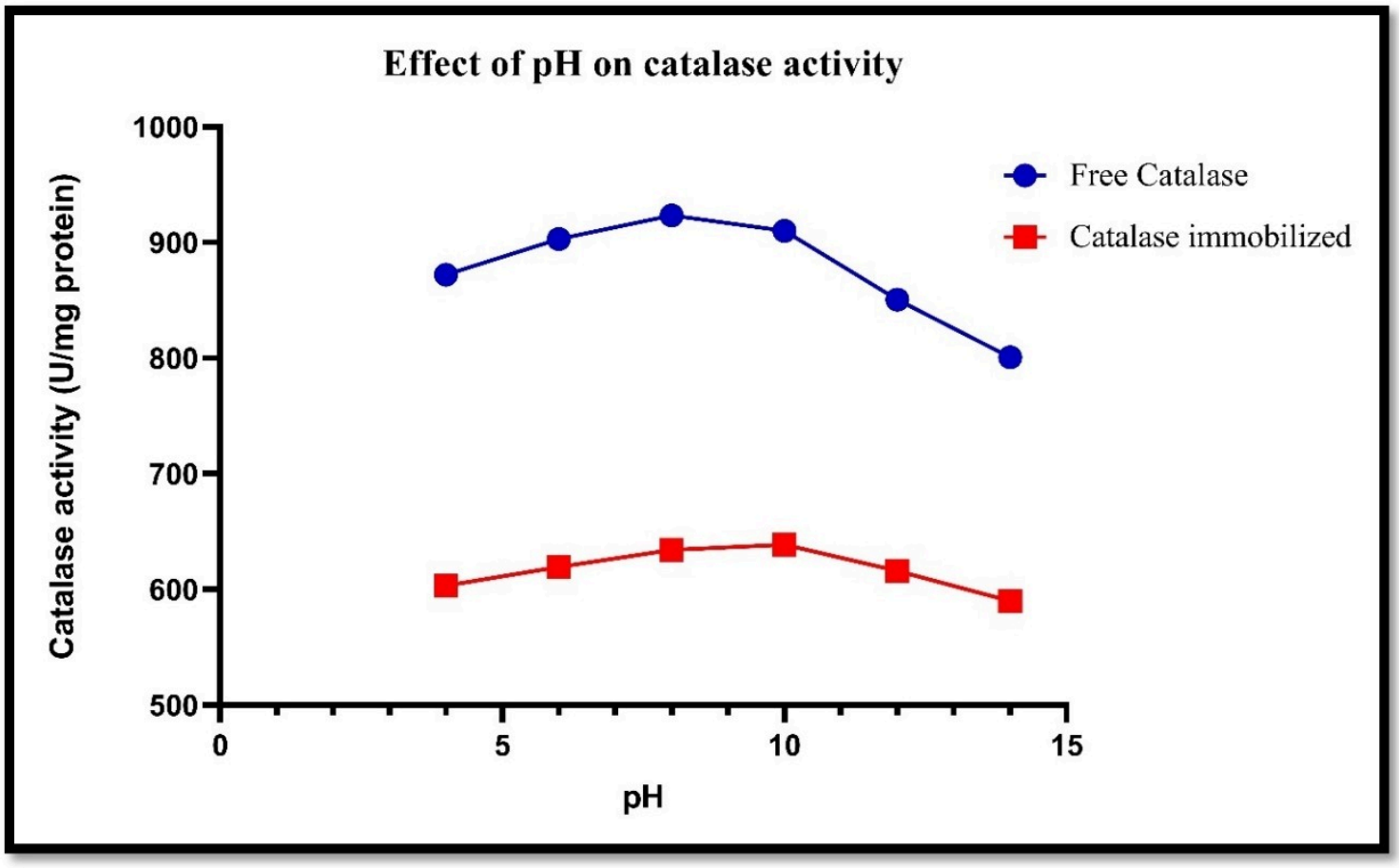


Figure 5

pH impact on free and immobilised catalase enzyme activity on iron oxide

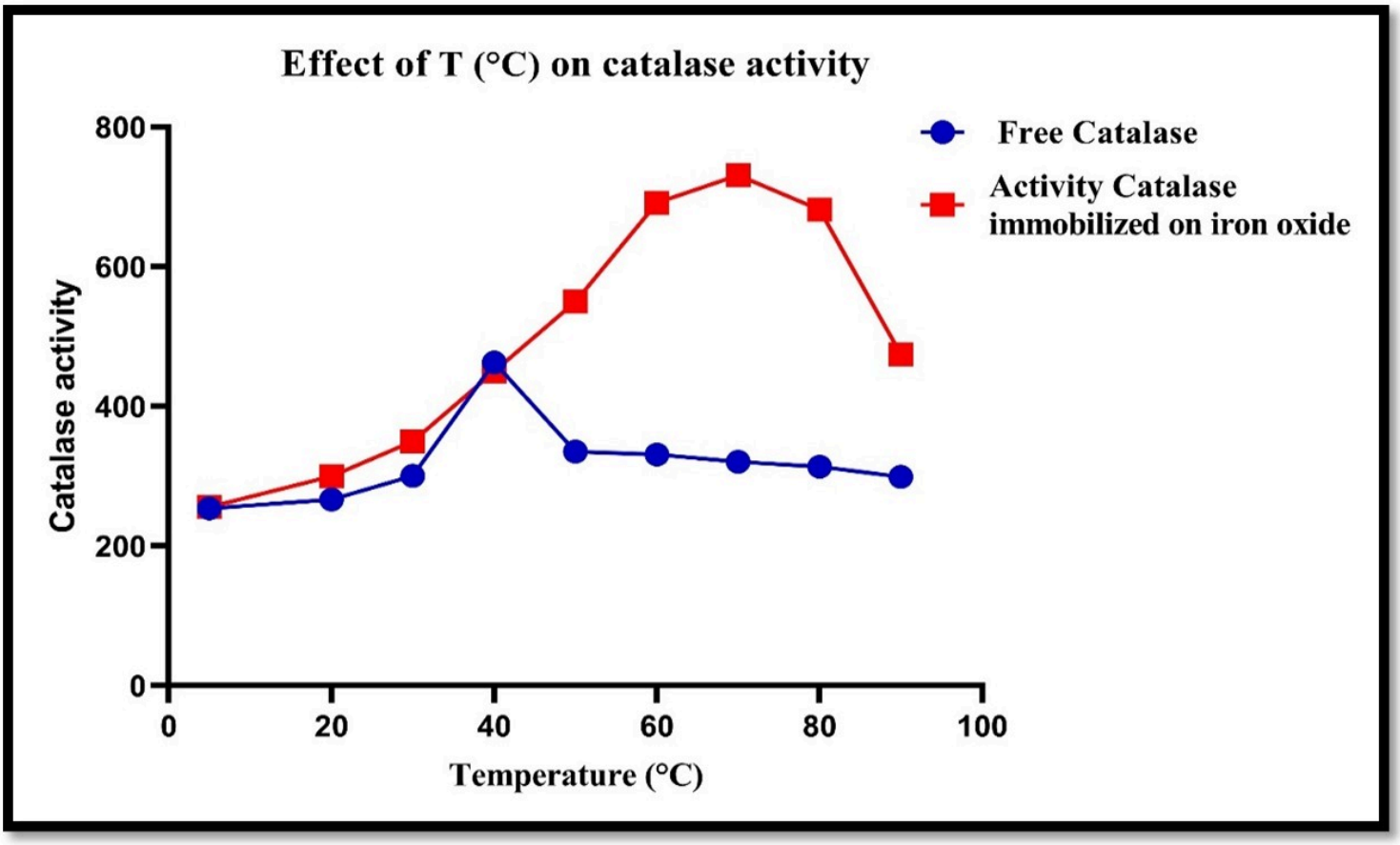


Figure 6

Temperature's impact on free and immobilised catalase enzyme activity on iron oxide

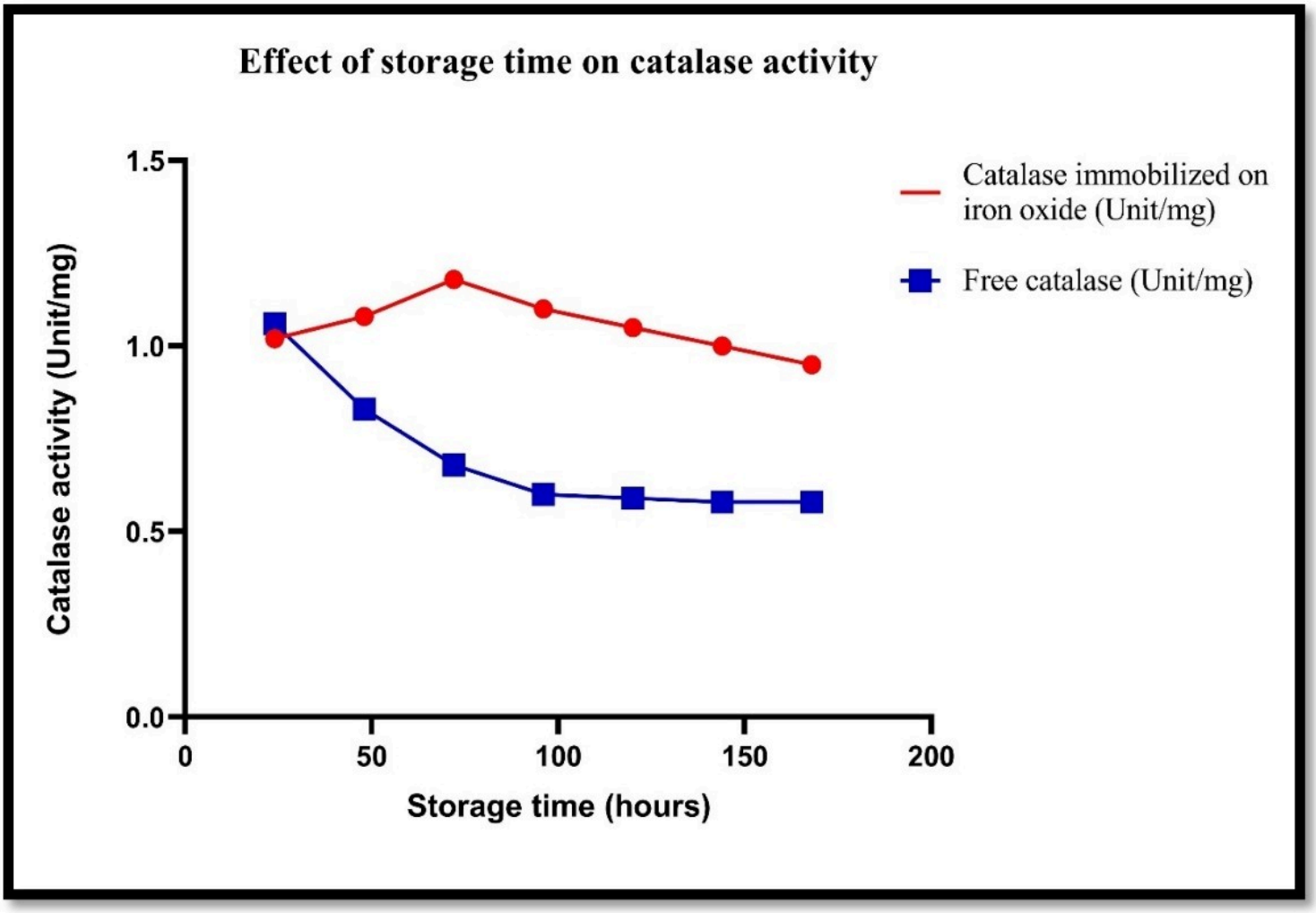


Figure 7

The impact of 168 hours of storage on the activity of fixed and free iron oxide catalase enzymes

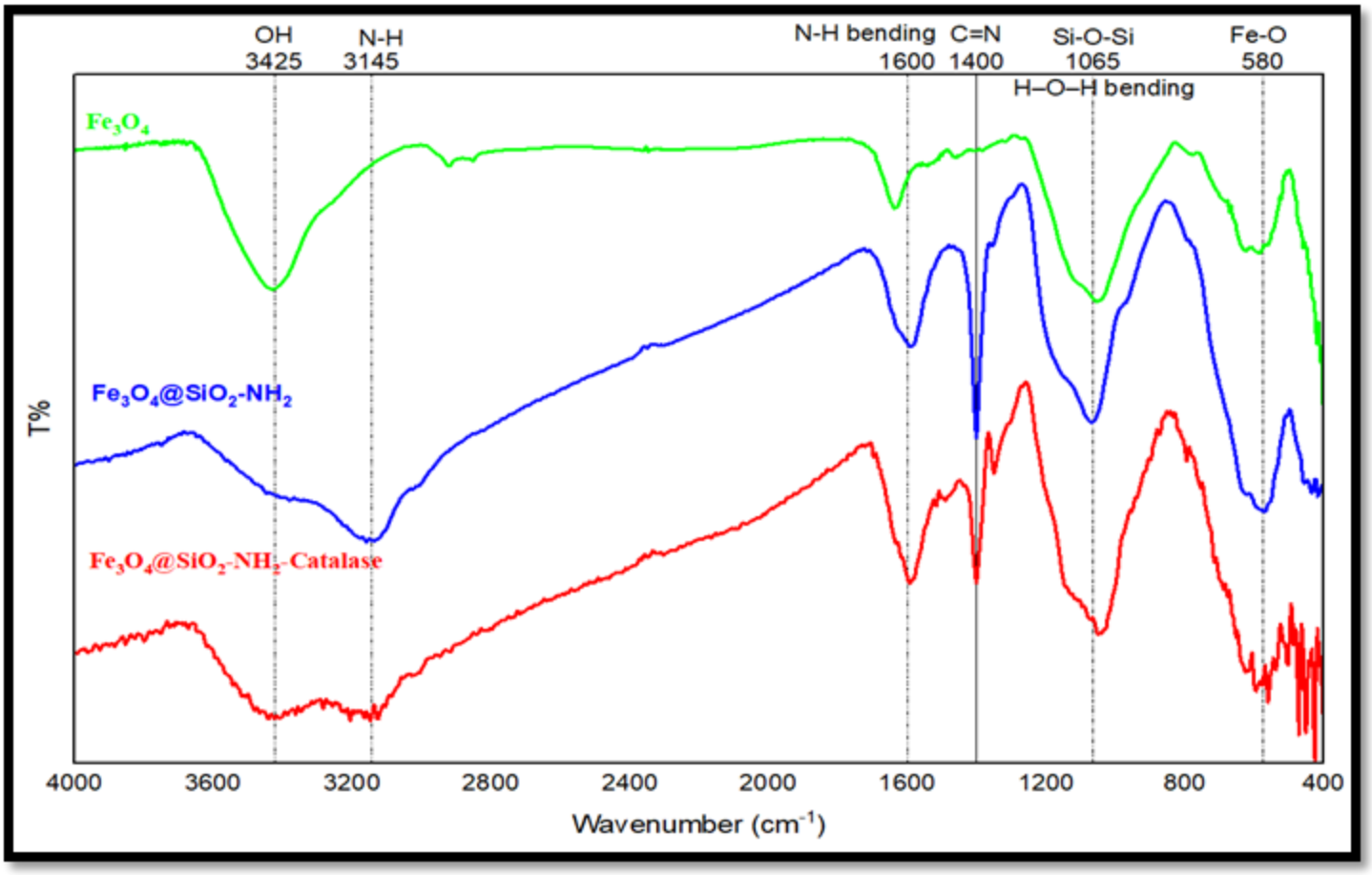


Figure 8

FTIR spectrum demonstrating catalase immobilisation and gradual surface change.

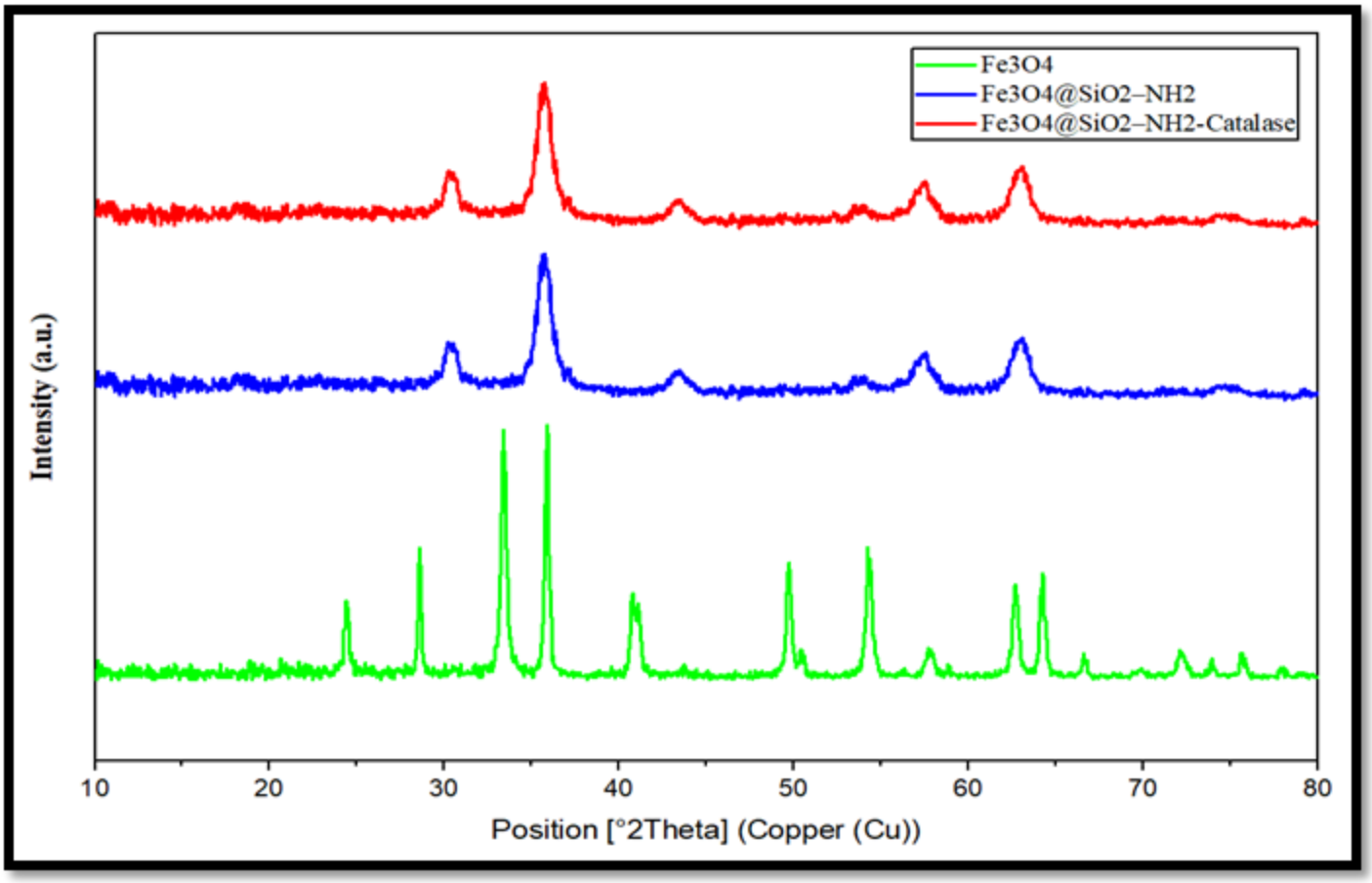


Figure 9

XRD patterns of Fe_3O_4, Fe_3O_4@SiO_2–NH_2, and Fe_3O_4@SiO_2–NH_2–CAT.

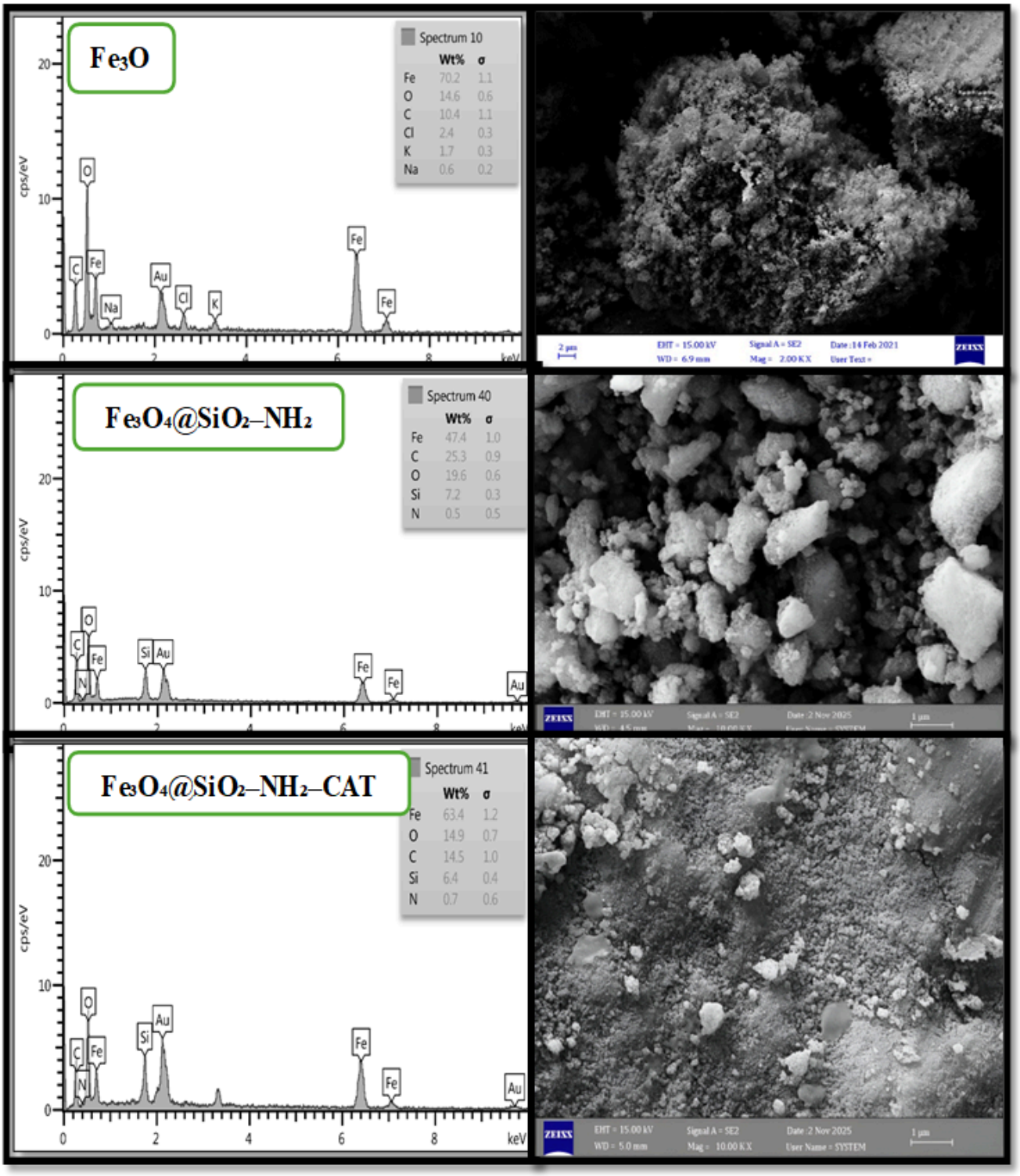


Figure 10

SEM images of Fe_3O_4, $Fe_3O_4@SiO_2–NH_2$, and $Fe_3O_4@SiO_2–NH_2–CAT$.

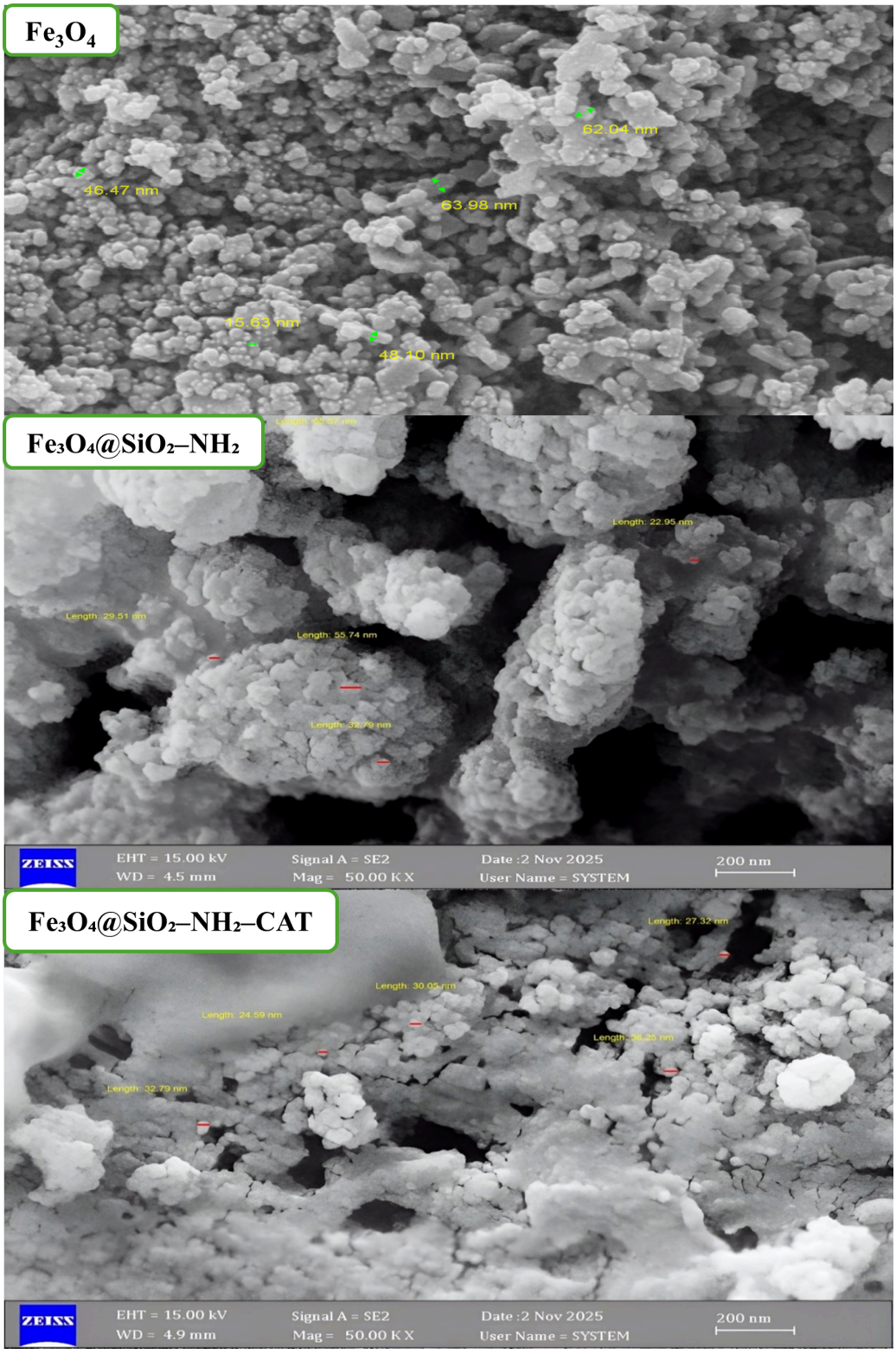


Figure 11

EDX spectra showing the elemental alterations related to catalase immobilization and surface modification.

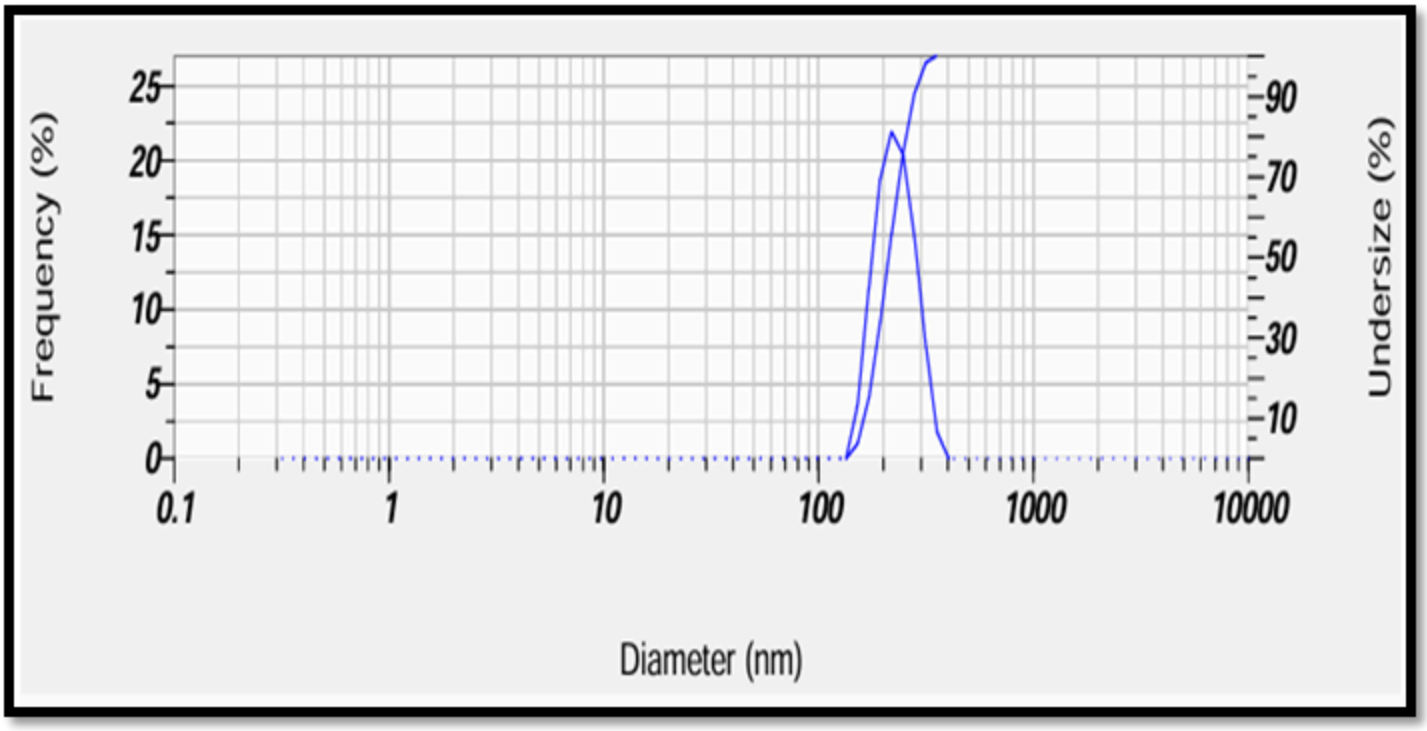


Figure 12

DLS profile of Fe_3O_4@SiO_2–NH_2–CAT showing hydrodynamic particle-size distribution.